

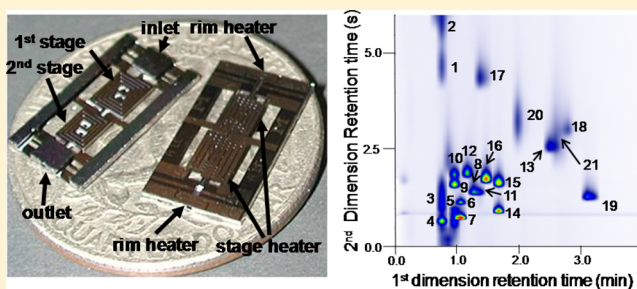
Comprehensive Two-Dimensional Gas Chromatographic Separations with a Microfabricated Thermal Modulator

Gustavo Serrano,^{†,‡,¶} Dibyadeep Paul,^{†,§,¶} Sung-Jin Kim,[¶] Katsuo Kurabayashi,^{*,†,§} and Edward T. Zellers^{*,†,‡,⊥}

[†]Center for Wireless Integrated MicroSensing and Systems, [‡]Department of Environmental Health Sciences, [§]Department of Mechanical Engineering, [¶]Department of Biomedical Engineering, and [⊥]Department of Chemistry, University of Michigan, Ann Arbor, Michigan 48109, United States

Supporting Information

ABSTRACT: Rapid, comprehensive two-dimensional gas chromatographic (GC × GC) separations by use of a microfabricated midpoint thermal modulator (μ TM) are demonstrated, and the effects of various μ TM design and operating parameters on performance are characterized. The two-stage μ TM chip consists of two interconnected spiral etched-Si microchannels (4.2 and 2.8 cm long) with a cross section of $250 \times 140 \mu\text{m}^2$, an anodically bonded Pyrex cap, and a cross-linked wall coating of poly(dimethylsiloxane) (PDMS). Integrated heaters provide rapid, sequential heating of each μ TM stage, while a proximate, underlying thermoelectric cooler provides continual cooling. The first-dimension column used for GC × GC separations was a 6 m long, $250 \mu\text{m}$ i.d. capillary with a PDMS stationary phase, and the second-dimension column was a 0.5 m long, $100 \mu\text{m}$ i.d. capillary with a poly(ethylene glycol) phase. Using sets of five to seven volatile test compounds (boiling point $\leq 174 \text{ }^\circ\text{C}$), the effects of the minimum (T_{min}) and maximum (T_{max}) modulation temperature, stage heating lag/offset (O_s), modulation period (P_M), and volumetric flow rate (F) on the quality of the separations were evaluated with respect to several performance metrics. Best results were obtained with a $T_{\text{min}} = -20 \text{ }^\circ\text{C}$, $T_{\text{max}} = 210 \text{ }^\circ\text{C}$, $O_s = 600 \text{ ms}$, $P_M = 6 \text{ s}$, and $F = 0.9 \text{ mL/min}$. Replicate modulated peak areas and retention times were reproducible to $<5\%$. A structured nine-component GC × GC chromatogram was produced, and a 21 component separation was achieved in $<3 \text{ min}$. The potential for creating portable $\mu\text{GC} \times \mu\text{GC}$ systems is discussed.



Numerous reports have appeared over the past decade or so on microscale gas chromatograph (μGC) components,^{1–13} subsystems,^{14–16} and systems,^{17–25} consisting of one or more microfabricated Si devices. The low power requirements, small size, and eventual low production cost of μGC systems favor their use in field or clinical settings for measuring volatile and semivolatile organic compounds (SVOC), such as explosive markers, chemical warfare agents, indoor air pollutants, and breath biomarkers of disease or toxic chemical exposure. Although the scaling laws governing GC separations generally favor miniaturization,²⁶ inherent limitations on the maximum length and minimum diameter of the (micro) columns, as well as the minimum injection bandwidth, place limits on the achievable peak capacity (n_p) and resolution (R_s). One approach to relieving these constraints on performance entails the use of comprehensive two-dimensional gas chromatography (GC × GC).

GC × GC is a highly effective method for separating the components of complex mixtures of (S)VOCs.²⁷ A junction-point modulator couples a relatively long first-dimension (^1D) column to a relatively short second-dimension (^2D) column having a different stationary phase and, thereby, different retention properties. As each compound elutes from the ^1D

column it is reinjected in a series of narrow bands that elute through the ^2D column rapidly enough to preserve the ^1D separation. Pneumatic modulation is achieved by tapping a second carrier gas source into the junction point and toggling a series of valves that transfer the effluent from the ^1D column to the ^2D column at very high frequency.^{28,29} Reinjection bandwidths as narrow as 22 ms can be obtained, but little or no focusing occurs, and therefore, the peak amplitude enhancement (PAE; i.e., the modulated/unmodulated peak height ratio) is generally quite limited.²⁹ Thermal modulation is achieved by alternately bathing a small section of capillary at the junction point in a cooled gas to trap and focus peak segments from the ^1D column and then heating to transfer them to the ^2D column.^{30–34} Reinjection bandwidths as narrow as 50 ms and PAE values as high as 70 have been reported by virtue of the refocusing that occurs with the thermal modulator (TM).^{27,32,33} Plotting the ^1D retention times against the ^2D retention times provides a two-dimensional (2-D) chromato-

Received: April 5, 2012

Accepted: July 19, 2012

Published: July 31, 2012

gram that conveys the net differential retention of the mixture components on the two columns.

The primary difficulties faced in trying to miniaturize GC \times GC systems with commercial TM subsystems are the need for large quantities of consumable cooling fluids and the power demands for both heating and cooling, which can be on the order of kilowatts.^{32b,33,34} As part of an ongoing effort concerned with the development of μ GC systems and components in our laboratories,^{1,4,7,8,14–16,18,21,22,24,25} we recently described a microfabricated TM (μ TM) that operates with relatively low power and without cryogenic fluids.^{35–37} The μ TM chip consists of two series-coupled, convolved-square-spiral, deep-reactive-ion-etched (DRIE) Si microchannels (stages) with an anodically bonded Pyrex cap, a cross-linked poly(dimethylsiloxane) (PDMS) wall coating, and individual thin-metal-film heaters and temperature sensors. The chip is mounted on a thermoelectric cooler (TEC), which is used for focusing. Highlights of that work include modulated peaks with full width at half-maximum (fwhm) values as low as 70 ms (for *n*-heptane) and PAE values as high as 50. Testing performed to date, however, entailed only a ¹D column so that the modulated peaks emerging from the μ TM could be characterized without the influence of a ²D column.

In this article, we describe a GC \times GC system that uses a μ TM of similar design to that reported previously. Relatively short commercial ¹D and ²D capillary columns are used in anticipation of developing a μ GC \times μ GC system for (S)VOCs. The effects of varying the stage temperatures, modulation period, stage-heating offset period, and volumetric flow rate are examined with respect to several performance metrics using a small set of VOCs as test analytes. The reproducibility of the 2-D separations provided under a given set of conditions is examined, and then a structured chromatogram is produced and assessed. Finally, a fast GC \times GC 21 component VOC mixture separation is presented. The implications of the results for using this type of μ TM in bench-scale GC \times GC systems and in portable μ GC \times μ GC systems for fast analysis of (S)VOC mixtures are considered.

EXPERIMENTAL SECTION

μ TM Preparation. The design, thermal analysis, and fabrication of the μ TM device have been described previously.^{35,36} Figure 1a shows a photograph of the device (see refs 35 and 36 for dimensional diagrams). The 13 \times 6 mm² μ TM chip consists of two square-spiral, boron-doped Si microchannels, 4.2 cm (stage 1) and 2.8 cm (stage 2) long, with cross sections of 250 μ m (*w*) \times 140 (*h*) μ m and wall thicknesses of 30 μ m. The microchannel dimensions were chosen on the basis of the modulator reported by Libardoni et al. in ref 34 and prior work by that group cited in that article. A 100 μ m thick Pyrex cap is anodically bonded to the top surface, sealing the microchannels and providing additional mechanical strength to the Si frame. There is a 0.5 mm long microchannel interconnection segment between the two stages. Connections to upstream and downstream capillaries are made at opposing sides of the rim. Four Ti/Pt resistive heaters and temperature sensors are patterned on the Pyrex surface, one set beneath each stage and another set beneath the inlet and outlet ports on the rim.

Two 5 cm long sections of deactivated fused-silica capillaries having 250 μ m i.d. and 100 μ m i.d. were connected to the inlet and outlet ports, respectively, with epoxy (Hysol epoxy patch 1C, Rocky Hill, CT). The interior walls of the microchannels

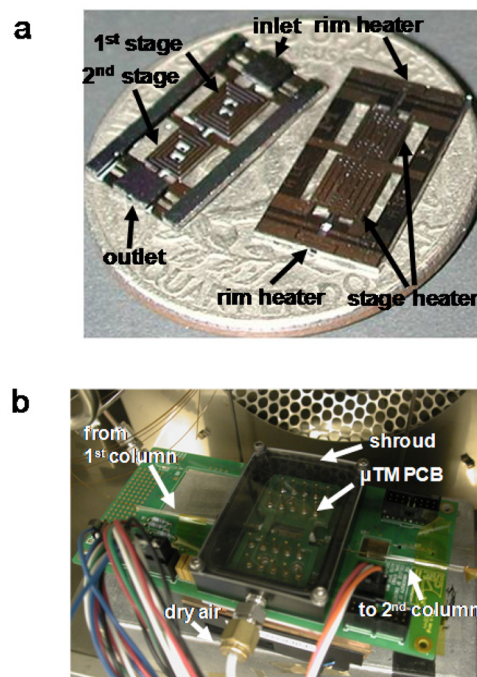


Figure 1. (a) Photograph of the microfabricated two-stage thermal modulator (μ TM), with labels identifying the essential features. (b) Photograph of the fully assembled μ TM mounted on a printed circuit board (PCB). The TEC is located beneath the μ TM PCB, and the ¹D and ²D columns are beyond the field of view.

(and connecting capillaries) were coated with a 0.3 μ m thick cross-linked film of PDMS (OV-1, Ohio Valley, Marietta, OH) from a 1:1 *n*-pentane/dichloromethane solution (0.6% w/v PDMS, 0.005% w/v dicumyl peroxide), using a static coating and thermal cross-linking method described previously.⁷ The μ TM chip was then mounted and wire-bonded to a custom printed circuit board in proximity to an underlying TEC as described in the Supporting Information accompanying this article.

Performance Testing. The μ TM-TEC testing platform was placed inside the oven of a bench-scale GC (model 6890, Agilent Technologies, Santa Clara, CA). Resistance values of the integrated temperature sensors were calibrated using the GC oven. The TEC was operated continuously at an applied power of 21 W, which yielded a minimum stage temperature, T_{\min} , of -40 $^{\circ}$ C with the rim heaters deactivated and an ambient temperature of 23 $^{\circ}$ C. Reducing the power to the TEC allowed for higher T_{\min} values. Modulations entailed applying 100 ms voltage pulses independently to each stage heater through two solid-state relays (D1D12, Crydom, San Diego, CA). The voltage applied to each stage was adjusted manually between 55 and 60 V to achieve the desired maximum stage temperature, T_{\max} , which ranged from 195 to 250 $^{\circ}$ C. A custom Visual C# program was used to control the timing of the applied voltages, as well as to read the temperature sensors via a DAQ card (NI USB-6212, National Instruments, Austin, TX) installed in a laptop computer. A constant voltage was applied independently to each rim heater and adjusted to maintain the ports at the ambient temperature when the TEC was on.

Inlet and outlet capillary sections were connected to commercial fused-silica capillary columns by means of press-tight connectors. The ¹D column was a 6 m long, 0.25 mm i.d. capillary with 0.25 μ m thick stationary phase of PDMS (Rtx-1,

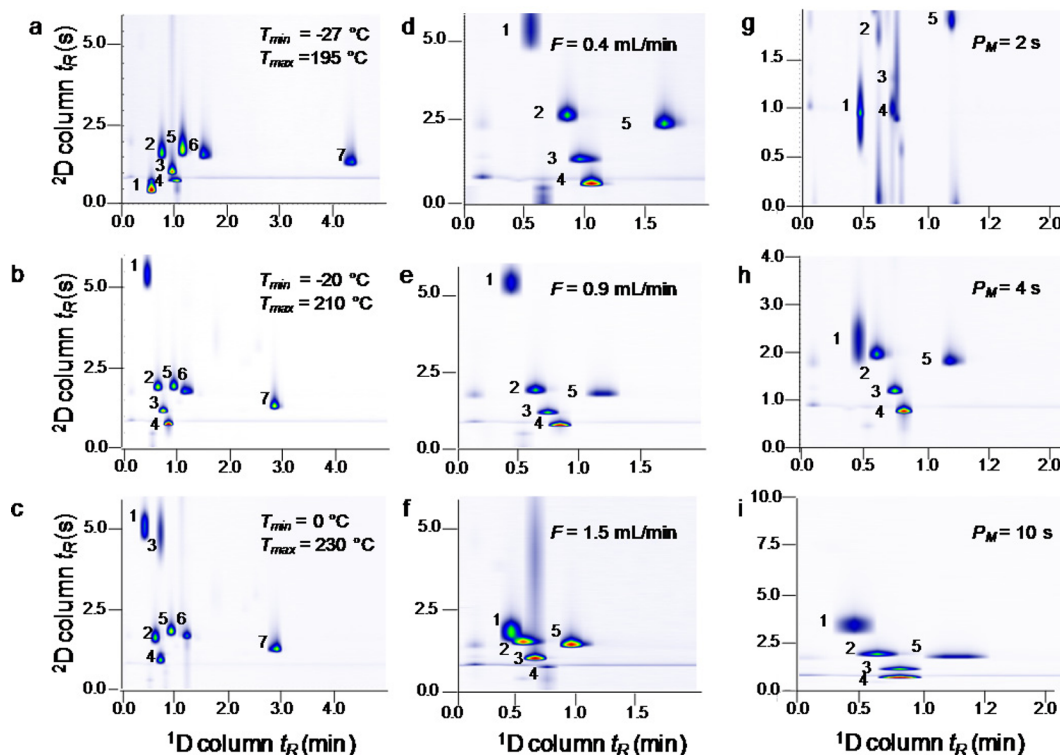


Figure 2. Two-dimensional chromatogram showing the effect of the modulator temperatures (a–c), volumetric flow rate (d–f), and modulation period (g–i) on the quality of separations; ^1D column temperature = $33\text{ }^\circ\text{C}$ ($25\text{ }^\circ\text{C}$ for panel a), ^2D column temperature = $80\text{ }^\circ\text{C}$. Conditions for panels a–c: $F = 0.9\text{ mL/min}$, $P_M = 6\text{ s}$, $O_s = 600\text{ ms}$. Conditions for panels d–f: $P_M = 6\text{ s}$, $O_s = 600\text{ ms}$, $T_{\min} = -20\text{ }^\circ\text{C}$, $T_{\max} = 210\text{ }^\circ\text{C}$. Conditions for panels g–i: $F = 0.9\text{ mL/min}$, $O_s = 600\text{ ms}$, $T_{\min} = -20\text{ }^\circ\text{C}$, $T_{\max} = 210\text{ }^\circ\text{C}$. Compounds: 1, benzene; 2, isoamyl alcohol; 3, hexanal; 4, *n*-octane; 5, 2-methyl-2-hexanol; 6, 2-heptanone; 7, *n*-decane.

Restek Corp., Bellefonte, PA), and the ^2D column was a 0.5 m long, 0.1 mm i.d. capillary with a 0.1 μm thick stationary phase of poly(ethylene glycol) (PEG, Rtx-Wax, Restek). The temperature of the ^1D column corresponded to that of the GC oven. The ^2D column was wrapped with insulated Cu wire (100 μm o.d., EIS, Inc., Atlanta, GA) and then with heat-resistant thin polyimide tape (McMaster Carr, Santa Fe Springs, CA). A fine-wire thermocouple (type K, Omega, Stamford, CT) was placed between the capillary and heater coil. For all tests the ^2D column was maintained at $\sim 80\text{ }^\circ\text{C}$. Note that the outlet capillary segment affixed to the μTM chip was coated with PDMS and was at oven temperature for all testing. The distal end of the ^2D column was connected to the flame ionization detector (FID) via a 5 cm segment of deactivated fused-silica capillary (100 μm i.d.). For some testing, the ^2D column was bypassed and the TEC was turned off so that the ^1D peak widths could be measured.

Test compounds were >98% pure (Sigma-Aldrich, Milwaukee, WI) and used without further purification. Vapor mixtures were prepared by injecting 1 μL of each component into a 10 L Tedlar bag (SKC Inc., Eighty-Four, PA) filled with a known volume of dry N_2 . A sample of this test atmosphere was drawn by a small diaphragm pump (UN86, KNF Neuberger, Trenton, NJ) through a 112 μL sampling loop connected to a six-port valve. The valve and loop were housed in a heated ($80\text{ }^\circ\text{C}$) enclosure on the GC chassis. Actuating the six-port valve injected the contents of the loop to the ^1D column of the GC \times GC subsystem via a short section of deactivated fused-silica capillary. Using He as the carrier gas, the volumetric flow rate, F , was adjusted by varying the GC inlet pressure and was

measured at the end of the ^2D column with a bubble flow meter.

The data sampling rate and temperature of the FID were 200 Hz and $250\text{ }^\circ\text{C}$, respectively. ChemStation software (rev.B.01.01, Agilent Technologies, Santa Clara, CA) was used for data acquisition, GRAMS32 (version 6.0, Thermo-Scientific, Pittsburgh, PA) was used for 1-D data processing, and GC Image (rev 2.2, Zoex, Houston, TX) was used for 2-D data processing and display of 2-D chromatograms.

RESULTS AND DISCUSSION

Several μTM operating variables must be set for a GC \times GC analysis, and each has an effect on performance. The stage-heating offset, O_s , is the time delay between heating of the first and second stage heaters, which can affect sample transfer efficiency. The modulation period, P_M , is the time between successive first-stage heating events (i.e., modulations), and it must be considered together with the retention time, t_R , on the ^2D column which, in turn, is affected by the F value, ^2D column temperature, and the analyte–stationary phase interactions. The values of T_{\min} and T_{\max} affect the efficiencies of trapping and remobilization, and the rates at which T_{\min} and T_{\max} are reached affect the minimum achievable P_M as well as the reinjection bandwidth for the ^2D column separation. The rate at which T_{\max} is reached for the μTM design used here is determined by the magnitude and duration of the applied heater voltage and was as high as $2300\text{ }^\circ\text{C/s}$ for the range of T_{\min} and T_{\max} values studied. The rate at which T_{\min} is reached is determined by the thermal mass of the stage and the net thermal resistance of all heat dissipation pathways.³⁵ Although

the thermal time constant for cooling the μ TM was ~ 0.34 s, regardless of T_{\max} , it required ~ 3 – 4 s to fully return to T_{\min} .

Thermal crosstalk between the rim and each stage and between the two stages can also affect performance. If no voltage were applied to the rim heaters, then the inlet and outlet ports would reach temperatures similar to T_{\min} , creating a cold spot in the sample transfer path. By applying a constant bias in the range of 2–3 V to each rim heater, the temperatures of the inlet and outlet ports were adjusted to match that of the GC oven (i.e., 25 or 33 °C). The interstage thermal crosstalk was ~ 7 – 10% for the μ TM design used in this study under the conditions employed. This is as much as 3% higher than that for the device described in ref 36 owing to the shorter interconnection microchannel employed (i.e., 0.5 vs 1 mm). As a result, heating the first stage led to a transient increase of ~ 16 – 19 °C in the value of T_{\min} for the second stage during each modulation over the ranges of T_{\max} and T_{\min} values studied. Increasing O_s from the default value of 600 to 1800 ms prolonged the transient temperature and reduced the trapping efficiency of the second stage. Reducing O_s to 200 ms gave performance similar to that for $O_s = 600$ ms, indicating that interstage heat transfer is rapid.

Performance was assessed with respect to the fwhm of the primary modulated peaks, the t_R values and critical-pair resolution in the 2D column (R_{s2}), the modulation ratio (M_R , i.e., number of detectable 2D peaks per 1D peak), n_p , and the extent of breakthrough. The latter phenomenon was assessed qualitatively by careful inspection of the 2-D chromatograms. Breakthrough occurs when the trapping capacity of the μ TM is exceeded in one or both stages. It is accompanied by the appearance of vertically broadened signals in the 2-D chromatogram at 1D retention times that are earlier than expected, and it results in unpredictable 2D retention times. Wrap-around occurs when P_M is shorter than the retention time on the 2D column. It results in compounds eluting in a later modulation cycle at an unpredictable, though reproducible, 2D retention time. R_{s2} is defined as $(t_{R2} - t_{R1})/w_A$, where t_{R2} and t_{R1} are the 2D retention times of adjacent compounds, assuming coelution in the first dimension, and w_A is the average base peak width of the primary modulated peaks.³⁸ Values of R_{s2} for the (“critical”) *n*-octane/hexanal pair were used to compare the performance under certain operating conditions.

The peak capacity represents the hypothetical number of perfectly spaced peaks that could be separated at a specified value of R_s : $n_p = 1 + N^{1/2}/(4R_s) \ln(t_{Ri}/t_M)$,³⁸ where N is the plate number derived from the expression $5.545(t_R/\text{fwhm})^2$, $R_s = 1$ for this study (arbitrary), t_M is the hold-up time, and t_{Ri} is the retention time of the last retained peak. For GC \times GC separations, $n_{p,\text{GC}\times\text{GC}}$ is the product of the peak capacity for each dimension, i.e., $n_{p1} \times n_{p2}$,²⁷ and P_M is used instead of t_{Ri} for the 2D column.³⁴

Modulator Temperatures. The influence of T_{\min} and T_{\max} on performance was evaluated using the following seven VOCs, the boiling points (bp) of which range from 80 to 174 °C: benzene, isoamyl alcohol, hexanal, *n*-octane, 2-methyl-2-hexanol, 2-heptanone, and *n*-decane. The values of O_s , P_M , and F used initially were 0.6 s, 6 s, and 0.9 mL/min, respectively. Four different combinations of T_{\min} and T_{\max} were tested; as the value of T_{\min} was adjusted the corresponding value of T_{\max} was also adjusted so as to maintain a span (i.e., $\Delta T = T_{\max} - T_{\min}$) of 220–230 °C.

For the first tests, with $T_{\min} = -27$ °C and $T_{\max} = 195$ °C, the 1D column temperature was 25 °C and the 2-D chromatogram

in Figure 2a was obtained. M_R values were between 2 and 3 for all compounds, all 2D t_R values were < 2.5 s, R_{s2} was 1.7, and the separation required 4.4 min. Importantly, the most volatile test compound, benzene, was trapped efficiently in the μ TM under these conditions. The 2D t_R values of the polar compounds were generally larger than those of the hydrocarbons, as expected, and the fwhm value of the primary modulated peak of each compound ranged from 82 ms (*n*-octane) to 300 ms (*n*-decane). The tailing observed along the 2D axis could arise from any of several of factors, including the low value of T_{\min} , the relatively thick PDMS wall coating in the μ TM, and the short segment of downstream interconnecting capillary, which was at the oven temperature of 25 °C. The horizontal band apparent in most of the Figure 2 panels has a retention time similar to that of *n*-octane in the 2D column and can be ascribed to a small amount of bleed arising from decomposition of the PDMS in the μ TM each time it is heated.

For the second test condition (Figure 2b), the GC oven (1D column and capillary interconnect) temperature was increased to 33 °C, and the lowest T_{\min} value that could be maintained was -20 °C. The value of T_{\max} was therefore increased to 210 °C. Under these conditions, breakthrough of benzene occurred; it eluted from the 2D column as a broadened signal in the modulation cycle preceding that in which it was expected and gave an anomalous 2D t_R value of ~ 5.4 s. This can be attributed to the interstage thermal crosstalk, which led to a transient increase in the second-stage T_{\min} value to -1 °C during each modulation and reduced the trapping capacity for benzene. The 2D t_R and M_R values of the remaining test compounds were similar to those in Figure 2a, but the 1D retention times were shorter due to the higher 1D column temperature. In addition, there was less 2D peak tailing due to the higher T_{\min} , T_{\max} , and interconnect temperatures; values of fwhm of the primary modulated peaks decreased slightly for the more volatile compounds (e.g., 72 ms for *n*-octane) and significantly for the less volatile compounds (e.g., 197 ms for *n*-decane). The R_{s2} value increased to 2.4 while the separation time decreased to 2.9 min.

For the data shown in Figure 2c, T_{\min} was increased to 0 °C (transient second-stage $T_{\min} = 16$ °C) and T_{\max} was increased to 230 °C while maintaining the column temperatures as in the previous run. In this case, both benzene and hexanal showed evidence of breakthrough from the second stage, and fwhm values increased 2–3-fold for all other compounds except *n*-decane, for which fwhm decreased by $\sim 10\%$ (i.e., 180 ms) in spite of the higher value of T_{\min} . Apparently, the increase in fwhm for the four other compounds arises from a reduction in focusing within the second stage of the modulator and a consequent increase in the reinjection bandwidth. Accordingly, the 2D t_R and M_R values and total separation time were the same as those for Figure 2b. Due to hexanal breakthrough, R_{s2} could not be calculated. The separation required < 3 min.

For $T_{\min} = 20$ °C (transient second-stage $T_{\min} = 35$ °C) and $T_{\max} = 250$ °C, all compounds except for *n*-decane broke through the modulator (data not shown). The fwhm of *n*-decane remained at 180 ms, suggesting that these conditions would be suitable for compounds of similar and somewhat lower volatility than *n*-decane. Note that the fwhm for *n*-decane did not change upon reducing T_{\max} to 210 °C, which indicates that the reinjection bandwidth was not limited by this factor.

From the preceding results, values of $T_{\min} = -20$ °C and $T_{\max} = 210$ °C seemed to provide the best performance for this set of compounds, with the exception of benzene. With these

modulator temperatures and the other operating conditions used in this series of experiments, $n_{p,GC \times GC}$ was 216 on the basis of the *n*-decane t_R and fwhm values ($n_{p1} = 18$; $n_{p2} = 12$) and 60 on the basis of 2-heptanone t_R and fwhm values (the latter allows comparisons with data from the next series of experiments).

Flow Rate. In GC \times GC, it is generally necessary to compromise between optimal carrier gas velocities for the 1D and 2D columns, because they are connected in series and F cannot be adjusted independently. In general, F should be adjusted such that the maximum 2D t_R value is less than P_M . This places a constraint on the minimum F value. At higher F values, several issues can arise. First, the trapping capacity of the modulator can be exceeded because of sample overloading or because insufficient time is available for the first stage to cool down after the first modulation heating event. Second, M_R values can be reduced because the peaks eluting from the 1D column are narrower.³⁹ Third, the retention on the 2D column could be reduced to a point where resolution is compromised. These factors, thus, place constraints on the maximum F value.

Golay plots generated separately for each column using He as carrier gas, (*n*-octane, $k = 2.7$, 33 °C for 1D ; and *n*-tridecane, $k = 2$, 80 °C for 2D) indicated optimal velocity values, u_{opt} of 37 and 14 cm/s for the 1D and 2D column, with H_{min} values of 0.028 and 0.017 cm, respectively. The corresponding values of N are 3570 and 5500 plates/m, respectively. This translates to F values of 1.2 mL/min for 1D column and 0.06 mL/min for 2D column. The effect of F was explored for a subset of five test compounds (i.e., benzene, isoamyl alcohol, hexanal, *n*-octane, and 2-heptanone) at discrete F values of 0.1, 0.4, 0.9, and 1.5 mL/min. Values of the other relevant operating variables are given in the caption of Figure 2.

As shown in the 2-D chromatograms in Figure 2d–f, increasing F leads to a commensurate decrease in the 1D column t_R values of all compounds. Notwithstanding the breakthrough of benzene under these conditions, the effects on the 2D column separation vary. At $F = 0.1$ mL/min the 2D t_R values exceeded P_M and all compounds exhibited wrap around; however, all compounds were well-separated (data not shown). Due to the broadness of the 1D peaks at this low flow rate, the M_R values were >3 and the separation required 4.4 min. The large fwhm values of the primary modulated peaks of the compounds are also attributed to the low F in the 2D column (e.g., *n*-octane fwhm = 627 ms).

At $F = 0.4$ mL/min (Figure 2d), all compounds were effectively separated in 1.6 min. R_{s2} was 2.7, M_R values ranged from 2.5 to 3.5, and the fwhm for the primary modulated peak of *n*-octane was 130 ms. On the basis of 2-heptanone, the $n_{p,GC \times GC}$ for this flow rate is 72 ($n_{p1} = 9$; $n_{p2} = 8$). At $F = 0.9$ mL/min (Figure 2e), the compounds were also effectively separated, R_{s2} was 2.5, M_R values ranged from 2 to 3, and the separation required 1.1 min. The fwhm for the primary modulated peak of *n*-octane was 76 ms. On the basis of 2-heptanone, the $n_{p,GC \times GC}$ for this modulation period is 60 ($n_{p1} = 6$ and $n_{p2} = 10$), slightly lower than at 0.4 mL/min. Increasing F to 1.5 mL/min (Figure 2f) led to very short t_R values on the 2D column. R_{s2} was not calculated due to breakthrough of hexanal; however, the resolution among the other compounds was lower than that at 0.9 mL/min. At this F , the base peak widths from the 1D column decreased to where M_R values were <2 . The separation required <1 min.

Although similar results were obtained for F values of 0.4 and 0.9 mL/min, the latter was deemed preferable because it

reduced the analysis time by 30% with minimal reductions in R_{s2} (8% reduction) and $n_{p,GC \times GC}$ (16% reduction).

Modulation Period. For the next series of tests, P_M was varied from 2 to 10 s while keeping all other variables at the same values as indicated for Figure 2e. The same subset of five test vapors was used. The shortest P_M value of 2 s (Figure 2g) resulted in breakthrough for all compounds due to insufficient time for cooling the μ TM stages between successive heating events. There was also evidence of wraparound for those compounds with t_R (2D) close to 2 s. At $P_M = 4$ s (Figure 2h), all compounds were effectively separated, R_{s2} was 2.4, M_R values ranged from 2.2 to 3, and the separation required 1.1 min. The fwhm for the primary modulated peak of *n*-octane was 80 ms. On the basis of 2-heptanone, the $n_{p,GC \times GC}$ for this modulation period is 57 ($n_{p1} = 6$; $n_{p2} = 9.5$). The data for $P_M = 6$ s was already presented in Figure 2e. R_{s2} was 2.2, M_R values ranged from 2.0 to 3.0, and the 2D t_R values were similar to those with $P_M = 4$ s. Despite the slightly smaller values of M_R and R_s , a P_M of 6 s is considered preferable to 4 s because it allows more time for the 2D separation and a slightly higher $n_{p,GC \times GC}$ (i.e., 60, based on 2-heptanone, see above).

At $P_M = 10$ s (Figure 2i), all compounds were effectively separated and only benzene suffered breakthrough. At this P_M value breakthrough might have been expected due to the limited capacity of the μ TM; however, none was observed for other compounds. R_{s2} was reduced to 1.6 and M_R values were <1.5 for all compounds, which is less than optimal, since the resolution in 2D is degraded. The separation required 1.1 min. The fwhm of the primary modulated peak of *n*-octane was 78 ms. The $n_{p,GC \times GC}$ value determined on the basis of 2-heptanone increases to 78 ($n_{p1} = 6$; $n_{p2} = 13$) mostly by virtue of using the value of P_M as the default retention time in the peak capacity calculation. It is clear from Figure 2i that one would want to operate at a lower flow rate to take full advantage of such a long P_M setting.

Reproducibility. To examine reproducibility, four replicate separations were performed for the same subset of five test compounds used in previous experiments under the conditions presented in Figure 2e. Table S1 (Supporting Information) shows the relative standard deviation (RSD) of the 2D t_R values and the total area of the modulated peaks. The former ranged from 2.2% for 2-heptanone to 4.6% for isoamyl alcohol and is largely a consequence of the lack of an automatic modulation event start timer for the GC \times GC analysis. The tailing peaks obtained for isoamyl alcohol in the 2D column contribute to its higher RSD value. The sums of the modulated peak areas show a similar degree of variability, with RSDs ranging from 1% to 5%. RSD values of the peak areas for individual modulated peaks, also shown in Supporting Information Table S1, are as high as 7%, undoubtedly due to changes in modulation phase associated with slight changes in the timing of the modulations.⁴⁰

Structured Chromatogram. Figure 3 shows more clearly the effect of the different stationary phases of the two columns. A mixture of 12 compounds composed of sets of *n*-alkanes (*n*-heptane, *n*-octane, *n*-nonane), aromatics (toluene, *m*-xylene, cumene), aldehydes (hexanal, heptanal, benzaldehyde), and alcohols (1-propanol, 1-hexanol, 2-heptanol) was separated using the conditions described above (see Figure 2e).

The alkanes eluted in order of bp from the 1D column and were well-separated, but they were not retained significantly on the polar 2D column. The aromatic compounds also eluted in order of bp from the 1D column and were retained only slightly

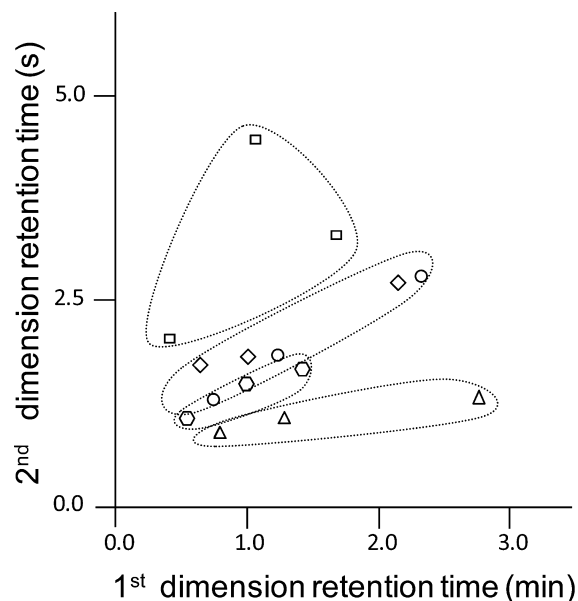


Figure 3. Structured chromatogram of compounds from several functional group classes. Symbols designate subsets: triangles for alkanes (in order of $^1\text{D } t_{\text{R}}$, *n*-heptane, *n*-octane, *n*-nonane); hexagons for aromatics (in order of $^1\text{D } t_{\text{R}}$, toluene, *m*-xylene, cumene); circles for ketones (in order of $^1\text{D } t_{\text{R}}$, 2-hexanone, cyclopentanone, 2-heptanone); diamonds for aldehydes (in order of $^1\text{D } t_{\text{R}}$, hexanal, heptanal, benzaldehyde); squares for alcohols (in order of $^1\text{D } t_{\text{R}}$, 1-propanol, 1-hexanol, 2-heptanol).

longer than the alkanes on the ^2D column, due to π - π interactions with the ether moieties on the PEG stationary phase of the ^2D column. The ketones and aldehydes also showed bp separations on the ^1D column and moderate retention on the ^2D column that reflects their relative polarities and the dominance of dipole-dipole interactions with the PEG. Note that several of these compounds coeluted with the aromatics and alkanes on the ^1D column, but they were separated on the ^2D column. As expected the alcohols, except for 1-propanol, had the largest t_{R} values on the ^2D column by virtue of strong dipolar and hydrogen-bonding interactions with the PEG. The relatively low $^2\text{D } t_{\text{R}}$ for 1-propanol can be explained by its high polarity and high volatility, which lead to second-stage breakthrough, as seen for benzene in previous experiments.

The grouping of homologues within a functional group class is a well-known feature/advantage of GC \times GC analyses of complex samples, where compound-specific analyses are often not necessary or feasible.²⁷ Although a high degree of orthogonality is observed between the ^1D and ^2D column separations, the increase in ^2D retention time with increasing carbon number within a homologous group reflects some residual volatility-based separation. This could be reduced or eliminated with temperature programming of the ^2D column.

Fast GC \times GC Separation of a Moderately Complex Mixture. Figure 4a shows the chromatogram from the ^1D column (i.e., bypassing the μTM and ^2D column) of a 21 component test mixture containing compounds spanning a bp range of 80 (benzene) to 178 °C (benzaldehyde). The column temperature was 33 °C, and F had to be increased to ~ 5 mL/min to obtain t_{R} values similar to those for the ^1D column obtained at 0.9 mL/min with the GC \times GC setup (Figure 4b). Peak assignments are based on individual runs of each

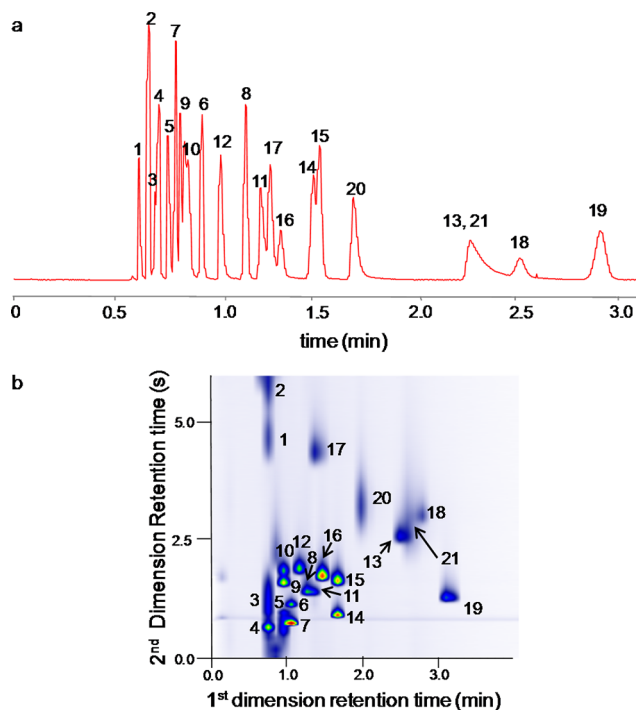


Figure 4. (a) One-dimensional chromatogram of a 21 component mixture (16–20 ng of each compound, injected as vapor). Conditions: 6 m, 0.25 mm i.d. PDMS (0.25 μm thickness); 33 °C (oven); $F = 5$ mL/min, FID. (b) GC \times GC chromatogram of the same mixture. The ^1D column was the same as used for the 1-D chromatogram (33 °C), the ^2D column was a 0.5 m, 0.10 mm i.d. PEG (0.10 μm thickness, 80 °C), $F = 0.9$ mL/min, $T_{\text{min}}/T_{\text{max}} = -20/210$ °C, $P_{\text{M}} = 6$ s, $O_{\text{s}} = 600$ ms, FID. Compounds (bp, °C): 1, benzene (80); 2, trichloroethylene (87); 3, 1-propanol (97); 4, *n*-heptane (98); 5, toluene (111); 6, hexanal (119–124); 7, *n*-octane (125); 8, 2-hexanone (127); 9, cyclopentanone (130); 10, isoamyl alcohol (131); 11, *m*-xylene (139); 12, 2-methyl-2-hexanol (141); 13, 2-heptanone (150); 14, *n*-nonane (151); 15, cumene (152); 16, heptanal (153); 17, 1-hexanol (155–159); 18, octanal (171); 19, *n*-decane (174); 20, 1-heptanol (175); 21, benzaldehyde (178).

component. The total analysis time was only 3 min. Overall, good peak shapes were obtained with some tailing of the more polar compounds. The following full or partially coelutions are apparent: peaks 3/4 (1-propanol/*n*-heptane), 9/10 (cyclopentanone/isoamyl alcohol), 14/15 (*n*-nonane/cumene), and 13/21 (2-heptanone/benzaldehyde). The n_{p} for this chromatogram is ~ 31 on the basis of the *n*-decane t_{R} value. Note that the relatively high value of F employed in this 1-D separation is well above the optimal value. However, operating at $F = 1.2$ mL/min (corresponding to u_{opt}) increased the total separation time 3-fold (i.e., to 9 min).

Figure 4b shows the GC \times GC chromatogram for the same mixture with the same modulator settings and operating conditions as used in the preceding section. Peaks 1, 2, and 3 correspond to the most volatile members of the mixture, benzene, trichloroethylene, and 1-propanol, respectively. They all showed evidence of breakthrough, as expected (vide supra). The peaks of the polar compounds (i.e., peaks 17, 18, 20, 13, and 21) were broader than those of the nonpolar compounds due to the longer $^2\text{D } t_{\text{R}}$ values. Values of fwhm of the primary modulated peaks ranged from 75 ms (*n*-heptane) to 900 ms (benzaldehyde). All of the overlapping peaks in the ^1D separation (Figure 4a) are resolved in the ^2D dimension;

however, peaks 8/11 (2-hexanone/*m*-xylene) are only partially resolved in the 2-D plot. The $n_{p,GC \times GC}$ is ~ 216 .

CONCLUSIONS

This is the first study to demonstrate GC \times GC separations with a μ TM. Short 1D and 2D columns were employed in anticipation of using microfabricated columns to assemble a μ GC \times μ GC system, which resulted in fast separations even for the moderately complex mixtures tested. The effects of the key operating variables T_{min} , T_{max} , O_s , P_m , and F on the quality of isothermal GC \times GC separations were rationalized in terms of the trapping capacity and transfer efficiency of the μ TM and the retention time on the 2D column. Results demonstrate that under proper operating conditions the performance of this robust μ TM rivals that of some commercial modulators requiring much higher operating power or consumable cryogenic fluids.

Due to the need to control the 1D column temperature by means of a conventional GC oven in this series of experiments, the lowest value of T_{min} achievable was limited by the oven temperature, which in turn reduced the trapping efficiency of the more volatile compounds tested. This problem will be easily resolved in the planned μ GC \times μ GC system by using on-chip heaters and temperature sensors to control the 1D and 2D microcolumn temperatures. Thermal crosstalk between stages also contributed to breakthrough of the more volatile compounds, and the relatively slow cooling time of the μ TM stages limited the minimum P_M to about 4 s. These issues should be resolved by increasing the length of the interstage interconnection channel and reducing the air gap between the μ TM and the TEC (at the cost of somewhat greater heating power dissipation), respectively.

Although a T_{max} of 210 °C was sufficient to remobilize even the least volatile compounds tested here, a higher T_{max} would be required to analyze mixtures containing components with boiling points >200 °C (e.g., essential oils, pesticides, and diesel fuel). Furthermore, progressive ramping of T_{min} and T_{max} would be required to analyze more complex mixtures. The former may require use of a different stationary phase in the modulator due to the possibility of excessive bleed at higher temperatures. The latter could be addressed by implementation of temperature controllers to coordinate T_{min} and T_{max} with the (micro)column temperature program over the course of the separation, while maintaining a constant value of ΔT .³³ These modifications would increase the range of compounds and the effective peak capacity of a μ GC \times μ GC system.

ASSOCIATED CONTENT

Supporting Information

Details about the μ TM mounting and the reproducibility of t_R values and areas of modulated peaks in the 2D column are presented. This material is available free of charge via the Internet at <http://pubs.acs.org>.

AUTHOR INFORMATION

Author Contributions

[¶]The first two authors contributed equally to this article.

Notes

The authors declare no competing financial interest.

ACKNOWLEDGMENTS

The authors thank Ken Wise for early project leadership, and Bruce Block and Robert Gordenker for their invaluable technical assistance. This project was supported by NASA under Grant NNG-06GA89G and by a gift from Agilent Technologies, and made use of Engineering Research Centers Shared Facilities supported by the National Science Foundation (NSF) under award no. EEC-0096866. Devices described herein were fabricated in the Lurie Nanofabrication Facility, a member of the National Nanotechnology Infrastructure Network, which is supported by NSF.

REFERENCES

- (1) Tian, W. C.; Chan, H. K. L.; Lu, C. J.; Pang, S. W.; Zellers, E. T. *J. Microelectromech. Syst.* **2005**, *14*, 498–507.
- (2) Manginell, R. P.; Akins, D. R.; Moorman, M. W.; Hadizadeh, R.; Copic, D.; Porter, D. A.; Anderson, J. M.; Hietala, V. M.; Bryan, J. R.; Wheeler, D. R.; Pfeifer, K. B.; Rumpf, A. *J. Microelectromech. Syst.* **2008**, *17*, 1396–1407.
- (3) Alfeeli, B.; Cho, D.; Ashraf-Khorassani, M.; Taylor, L. T.; Agah, M. *Sens. Actuators, B* **2008**, *133*, 24–32.
- (4) Reidy, S.; Lambertus, G.; Reece, J.; Sacks, R. *Anal. Chem.* **2006**, *78*, 2623–2630.
- (5) Radadia, A. D.; Masel, R. I.; Shannon, M. A.; Jerrell, J. P.; Cadwallader, K. R. *Anal. Chem.* **2008**, *80*, 4087–4094.
- (6) Zarejan-Jahromi, M. A.; Ashraf-Khorassani, M.; Taylor, L. T.; Agah, M. *J. Microelectromech. Syst.* **2009**, *18*, 28–37.
- (7) Serrano, G.; Reidy, S. M.; Zellers, E. T. *Sens. Actuators, B* **2009**, *141*, 217–226.
- (8) Cai, Q. Y.; Zellers, E. T. *Anal. Chem.* **2002**, *74*, 3533–3539.
- (9) Jian, R.-S.; Huang, R.-X.; Lu, C.-J. *Talanta* **2012**, *88*, 160–167.
- (10) Li, M.; Myers, E. B.; Tang, H. X.; Aldridge, S. J.; McCaig, H. C.; Whiting, J. J.; Simonson, R. J.; Lewis, N. S.; Roukes, M. L. *Nano Lett.* **2010**, *10*, 3899–3903.
- (11) Reddy, K.; Guo, Y.; Liu, J.; Lee, W.; Oo, M. K. K.; Fan, X. D. *Sens. Actuators, B* **2011**, *159*, 60–65.
- (12) Cruz, D.; Chang, J. P.; Showalter, S. K.; Gelbard, F.; Manginell, R. P.; Blain, M. G. *Sens. Actuators, B* **2007**, *121*, 414–422.
- (13) Galambos, P.; Lantz, J.; Baker, M. S.; McClain, J.; Bogart, G. R.; Simonson, R. J. *J. Microelectromech. Syst.* **2011**, *20*, 1150–1162.
- (14) Lambertus, G. R.; Fix, C. S.; Reidy, S. M.; Miller, R.; Wheeler, D.; Nazarov, E.; Sacks, R. D. *Anal. Chem.* **2005**, *77*, 7563–7571.
- (15) Serrano, G.; Chang, H.; Zellers, E. T. *Proceedings of Transducers '09*, Denver, CO, June 2009; pp 1654–1657.
- (16) Kim, S. K.; Chang, H.; Zellers, E. T. *Proceedings of Transducers '09*, Denver, CO, June 21–25, 2009; pp 719–723.
- (17) Canary-Three, Defiant Technologies. <http://www.defiant-tech.com/canarythree.php> (accessed February 2012).
- (18) Lu, C. J.; Steineker, W.; Tian, W. C.; Oborny, M.; Nichols, J.; Agah, M.; Potkay, J.; Chang, H.; Driscoll, J.; Sacks, R.; Wise, K.; Pang, S.; Zellers, E. T. *Lab Chip* **2005**, *5*, 1123–1131.
- (19) Lewis, P. R.; Manginell, R. P.; Adkins, D. R.; Kottenstette, R. J.; Wheeler, D.; Sokolowski, S.; Trudell, D. E.; Bymes, J.; Okandan, M.; Bauer, J. M.; Manley, R. G.; Frye-Mason, G. C. *IEEE Sens. J.* **2006**, *6*, 784–795.
- (20) Zampolli, S.; Elmi, I.; Mancarella, F.; Betti, P.; Dalcanale, E.; Cardinali, G. C.; Severi, M. *Sens. Actuators, B* **2009**, *141*, 322–328.
- (21) Zellers, E. T.; Serrano, G.; Chang, H.; Amos, L. K. *Proceedings of Transducers '11*, Beijing, China, June 5–9; pp 2082–2085.
- (22) Kim, S. K.; Chang, H.; Zellers, E. T. *Anal. Chem.* **2011**, *83*, 7198–7206.
- (23) Manginell, R. P.; Bauer, J. M.; Moorman, M. W.; Sanchez, L. J.; Anderson, J. M.; Whiting, J. J.; Porter, D. A.; Copic, D.; Achyuthan, K. E. *Sensors* **2011**, *11*, 6517–6532.
- (24) Kim, S. K.; Burris, D. R.; Chang, H.; Bryant-Genevier, J.; Zellers, E. T. *Environ. Sci. Technol.* **2012**, *46*, 6065–6072.

- (25) Kim, S. K.; Burriss, D. R.; Chang, H.; Bryant-Genevier, J.; Gorder, K. A.; Dettenmaier, E. M.; Zellers, E. T. *Environ. Sci. Technol.* **2012**, *46*, 6073–6080.
- (26) Reid, V. R.; Synovec, R. E. *Talanta* **2008**, *76*, 703–717.
- (27) Dalluge, J.; Beens, J.; Brinkman, U. T. J. *Chromatogr., A* **2003**, *1000*, 69–108.
- (28) Mohler, R. E.; Prazen, B. J.; Synovec, R. E. *Anal. Chim. Acta* **2006**, *555*, 68–74.
- (29) Seeley, J. V.; Micyus, N. J.; Bandurski, S. V.; Seeley, S. K.; McCurry, J. D. *Anal. Chem.* **2007**, *79*, 1840–1847.
- (30) Philips, J. B.; Gaines, R. B.; Blomberg, J.; Van der Wielen, F. W. M.; Dimandja, J. M.; Green, V.; Granger, J.; Patterson, D.; Racovalis, L.; de Geus, H. J.; de Boer, J.; Haglund, P.; Lipsky, J.; Sinha, V.; Ledford, E. B. J. *High Resolut. Chromatogr.* **1999**, *22*, 3–10.
- (31) Adahchour, M.; Beens, J.; Brinkman, U. A. T. *Analyst* **2003**, *128*, 213–216.
- (32) (a) Harynuk, J.; Gorecki, T. J. *Chromatogr., A* **2003**, *1019*, 53–63. (b) Panic, O.; Gorecki, T.; McNeish, C.; Goldstein, A. H.; Williams, B. J.; Worton, D. R.; Hering, S. V.; Kreisberg, N. H. J. *Chromatogr., A* **2011**, *1218*, 3070–3079.
- (33) Begnaud, F.; Debonneville, C.; Probst, J.-P.; Chaintreau, A.; Morrison, P. D.; Adcock, J. L.; Marriott, P. J. *J. Sep. Sci.* **2009**, *32*, 3144–3151.
- (34) Libardoni, M.; Fix, C.; Waite, J. H.; Sacks, R. *Anal. Methods* **2010**, *2*, 936–943.
- (35) Kim, S.-J.; Reidy, S. M.; Block, B. P.; Wise, K. D.; Zellers, E. T.; Kurabayashi, K. *Lab Chip* **2010**, *10*, 1647–1654.
- (36) Kim, S.-J.; Serrano, G.; Wise, K. D.; Kurabayashi, K.; Zellers, E. T. *Anal. Chem.* **2011**, *83*, 5556–5562.
- (37) Paul, D.; Serrano, G.; Zellers, E. T.; Kurabayashi, K. *Proceedings of MEMS '12*, Paris, France, Jan 29–Feb 2, 2012; pp 96–99.
- (38) Grob, R. L. *Modern Practice of Gas Chromatography*, 3rd ed.; Wiley-Interscience: New York, 2005; Chapter 3.
- (39) Khummueng, W.; Harynuk, J.; Marriott, P. J. *Anal. Chem.* **2006**, *78*, 4578–4587.
- (40) Shellie, R. A.; Xie, L.-L.; Marriott, P. J. *J. Chromatogr., A* **2002**, *968*, 161–170.